

## Circulating LL37 targets plasma extracellular vesicles to immune cells and intensifies Behçet's disease severity

Tamer Kahraman, Gozde Gucluler, Ismail Simsek, Fuat Cem Yagci, Muzaffer Yildirim, Can Ozen, Ayhan Dinc, Mayda Gursel, Lolai Ikromzoda, Tolga Sutlu, Stephen Gay & Ihsan Gursel

To cite this article: Tamer Kahraman, Gozde Gucluler, Ismail Simsek, Fuat Cem Yagci, Muzaffer Yildirim, Can Ozen, Ayhan Dinc, Mayda Gursel, Lolai Ikromzoda, Tolga Sutlu, Stephen Gay & Ihsan Gursel (2017) Circulating LL37 targets plasma extracellular vesicles to immune cells and intensifies Behçet's disease severity, Journal of Extracellular Vesicles, 6:1, 1284449

To link to this article: <https://doi.org/10.1080/20013078.2017.1284449>



© 2017 The Author(s). Published by Informa UK Limited, trading as Taylor & Francis Group.



[View supplementary material](#)



Published online: 28 Feb 2017.



[Submit your article to this journal](#)



Article views: 481



[View related articles](#)



[View Crossmark data](#)

## Circulating LL37 targets plasma extracellular vesicles to immune cells and intensifies Behçet's disease severity

Tamer Kahraman<sup>a\*</sup>, Gozde Gucluler<sup>a\*</sup>, Ismail Simsek<sup>b</sup>, Fuat Cem Yagci<sup>a</sup>, Muzaffer Yildirim<sup>a</sup>, Can Ozen<sup>c</sup>, Ayhan Dinc<sup>b</sup>, Mayda Gursel<sup>d</sup>, Lolai Ikromzoda<sup>e</sup>, Tolga Sutlu<sup>e</sup>, Stephen Gay<sup>f</sup> and Ihsan Gursel<sup>a</sup>

<sup>a</sup>Science Faculty, Department of Molecular Biology and Genetics, Bilkent University, Ankara, Turkey; <sup>b</sup>Division of Rheumatology, Gulhane School of Medicine, Ankara, Turkey; <sup>c</sup>Department of Biotechnology, Middle East Technical University, Ankara, Turkey; <sup>d</sup>Department of Biological Sciences, Middle East Technical University, Ankara, Turkey; <sup>e</sup>Nanotechnology Research and Application Center, Sabanci University, Istanbul, Turkey; <sup>f</sup>Department of Rheumatology, University Hospital Zurich, Zurich, Switzerland

### ABSTRACT

Behçet's disease (BD) activity is characterised by sustained, over-exuberant immune activation, yet the underlying mechanisms leading to active BD state are poorly defined. Herein, we show that the human cathelicidin derived antimicrobial peptide LL37 associates with and directs plasma extracellular vesicles (EV) to immune cells, thereby leading to enhanced immune activation aggravating BD pathology. Notably, disease activity was correlated with elevated levels of circulating LL37 and EV plasma concentration. Stimulation of healthy PBMC with active BD patient EVs induced heightened IL1 $\beta$ , IFN $\alpha$ , IL6 and IP10 secretion compared to healthy and inactive BD EVs. Remarkably, when mixed with LL37, healthy plasma-EVs triggered a robust immune activation replicating the pathology inducing properties of BD EVs. The findings of this study could be of clinical interest in the management of BD, implicating LL37/EV association as one of the major contributors of BD pathogenesis.

**Abbreviations:** BD: Behçet's disease; EV: extracellular vesicle; BB: binding buffer; AnV: annexin V; autologEV: autologous extracellular vesicles; alloEV: allogeneic extracellular vesicles

### ARTICLE HISTORY

Received 4 March 2016  
Revised 28 November 2016  
Accepted 3 December 2016

### RESPONSIBLE EDITOR

Edit Buzás, Semmelweis University, Hungary

### KEYWORDS

Extracellular vesicles; Behçet's disease; autoimmune; immune activation; LL37; cytokine

## Introduction

Behçet's disease (BD) is a complex multi-organ chronic inflammatory condition of unknown etiology wherein the genetic background and environmental factors are thought to be important contributors for disease pathogenesis.[1–5] Recent findings suggest that a predominance of Th1/Th17-type immune polarisations and elevated levels of associated cytokines correlate with disease activity.[6–9] In this context, plasmapheresis has been shown to induce rapid short-term remission suggesting that an unidentified plasma-associated factor could be a trigger of flare-ups.[10] Herein, we hypothesised that one such plasma-related factor contributing to disease activity and severity could be the circulating extracellular vesicles (EV).

EVs are small vesicles (diameter of 30 nm to 1  $\mu$ m) constitutively released from various cell types and are considered as key players mediating cell-to-cell communication.[11–13] Accumulating evidence suggests that plasma EV levels are altered during disease states.[12] For instance, the number of EVs released from cultured immune cells increases dramatically upon stimulation


with TNF $\alpha$  or IL1 $\beta$ . Moreover, several apoptosis inducers contribute to EV secretion.[13–17] In addition, stimulation of RAW 264.7 cells by TLR ligands intensify EV release.[18] EVs have several roles in immune modulation along with stimulation of coagulation, and modulation of vascular functions.[19–25] In general, their cargo is loaded with an array of bioactive molecules capable of regulating target cell behaviour.[23–27] Recent studies revealed that numbers of circulating EVs were elevated in several rheumatologic diseases, such as rheumatoid arthritis, systemic lupus erythematosus, primary Sjögren's syndrome, vasculitis and anti-phospholipid syndrome.[20–31] The implications of elevated EV levels were not fully understood.

Since inflammation, endothelial dysfunction, and thrombotic tendency are collectively regarded as cardinal features of BD, we speculated that the levels and source of EVs along with their cargo might influence the course of BD in terms of disease activity and severity.

In this study, we report that circulating EV numbers correlate with BD severity. Furthermore, we show that

**CONTACT** Ihsan Gursel  [ihsangursel@bilkent.edu.tr](mailto:ihsangursel@bilkent.edu.tr)

\*These authors contributed equally.

 Supplemental data for this article can be accessed [here](#).

© 2017 The Author(s). Published by Informa UK Limited, trading as Taylor & Francis Group.

This is an Open Access article distributed under the terms of the Creative Commons Attribution-NonCommercial License (<http://creativecommons.org/licenses/by-nc/4.0/>), which permits unrestricted non-commercial use, distribution, and reproduction in any medium, provided the original work is properly cited.

the human cathelicidin group of anti-microbial peptide LL37 associates with EVs, enhancing their internalisation by immune cells, initiating a robust pro-inflammatory cytokine milieu.

## Materials and methods

### Patients and controls

Consecutive patients, who were regularly examined at the Department of Rheumatology and had an established diagnosis of BD (according to the criteria of the International Study Group for Behçet's Disease [32]), were referred for the study after they had their last clinical evaluation to determine clinical disease status (see Table 1). For this study, plasma of 72 BD patients (active;  $n = 35$ , inactive;  $n = 37$ ) and 22 healthy control individuals were included. Patients having active disease was defined by the presence of two and more clinical characteristics, such as oral ulcers, genital ulcers, papulopustular or pseudo-follicular cutaneous lesions, active vascular disease and active ocular involvement. The patients who had no symptoms related with BD at the time of sampling and receiving steady medication for at least one month were classified as having an inactive disease. All patients were further categorised according to their organ of involvement as (i) mucocutaneous, (ii) ocular, and (iii) vascular. With regard to the classification of those patients with inactive disease, patients' detailed clinical history was investigated with respect to either deep vein thrombosis or arterial aneurysm and evidence for uveitis was sought. Subjects with hypertension, diabetes mellitus, renal disease or a previous history of coronary artery disease or myocardial infarction were excluded. The healthy control group included 22 individuals, matched for age and sex. Baseline characteristics of patients with BD and healthy subjects at inclusion are summarised in Table 1. The study was approved by the Institutional Review Board, and all participants provided their informed consents.

**Table 1.** Clinical evaluations of the BD patients.

	Healthy ( $n = 22$ )	Inactive BD ( $n = 37$ )	Active BD ( $n = 35$ )
Sex (M)	22	37	35
Age (year, mean $\pm$ SD)	22 $\pm$ 5	22 $\pm$ 5	19 $\pm$ 6
Disease duration (year, mean $\pm$ SD)	N/A	11 $\pm$ 5	8 $\pm$ 2
<b>Disease progression</b>			
Mucosa	N/A	9	16
Vein	N/A	12	7
Eye	N/A	16	12
<b>Treatment</b>			
Colchicine	N/A	21	24
Azathioprine	N/A	14	11
Cyclophosphamide	N/A	2	0

### Collection of platelet poor plasma from PBMCs

Fresh blood samples collected into sodium citrate containing vacutainers were centrifuged at 400g for 10 min; plasma was separated and further centrifuged at 1500g for 10 min to obtain platelet poor plasma (PPP). The PPP was collected and divided into 1.5 ml aliquots, which were snap-frozen in liquid nitrogen and kept at  $-80^{\circ}\text{C}$ .

### Isolation of EVs by differential centrifugation

EV isolation from PPP was based on the differential centrifugation method.[33] All reagents used throughout the purification were filtered using 0.2  $\mu\text{m}$  filters and then centrifuged at 100,000g for two hours. Briefly, PPPs were thawed centrifuged at 10,000g for 10 min to remove cell debris. One ml of the supernatant was 35 $\times$  diluted by PBS-citrate buffer (10 mM tri-sodium citrate in  $\text{Ca}^{2+}/\text{Mg}^{2+}$  free PBS, pH = 7.4) and centrifuged at 100,000g for 1 h (XL90 Beckman ultracentrifuge with a SW28 rotor with 6  $\times$  38.5 ml polyallomer tubes, Beckman Instruments, Fullerton, CA, USA). The supernatant was discarded, and the pellet was washed once with PBS-citrate buffer. The pellet (containing EV fraction) was then dissolved in 150  $\mu\text{l}$  of buffer, either 1 $\times$  PBS or binding buffer (BB) (10 $\times$  BB was composed of 0.1 M HEPES, 1.4 M NaCl and 25 mM  $\text{CaCl}_2$ , pH = 7.4).

### Purification of EVs by sucrose cushion

Purification of EVs using sucrose cushion was performed as described elsewhere.[33] The isolated EV pellet, after the final ultracentrifugation step, was dissolved in 2 ml 1 $\times$  PBS. The EVs were then added to 30% (w/v) sucrose solution in 15 ml ultracentrifuge UC polyallomer tubes and centrifuged for 2 h at 100,000g. After centrifugation, 3–4 ml of supernatant (including purified EVs) from the top of the sucrose solution was collected and transferred into 38.5 ml UC polyallomer tubes. Up to 35 ml 1 $\times$  PBS was added onto the solution and centrifuged for 2 h at 100,000g. The EV pellet was collected by using 150  $\mu\text{l}$  1 $\times$  PBS for subsequent analysis.

### Characterisation of EVs by western blotting

EVs for western blotting was prepared with RIPA lysis buffer and protein concentration was determined using BCA Protein Assay Reagent Kit (Thermo Scientific, Waltham, MA, USA). An amount of 25  $\mu\text{g}$  of protein was loaded and separated by SDS-polyacrylamide gel electrophoresis, transferred to PVDF membrane and probed with 1:1000 diluted primary antibodies against Alix (Cell Signaling, Denver, CO, USA) and Grp94 (Cell

Signaling). Blots were visualised by Amersham Imager 600 (GE, Amersham, UK) after incubating membranes with 1:10,000 diluted HRP linked secondary antibodies as anti-mouse IgG (Cell Signaling) and anti-rabbit IgG (Cell Signaling) for Alix and Grp94 blotting, respectively.

### **Characterisation of EV markers with bead assay using flow cytometer**

In order to characterise exosomal surface antigens by flow cytometer, initially, 10  $\mu\text{l}$  carboxyl modified latex beads (bead diameter: 3.9  $\mu\text{m}$ , Invitrogen, Carlsbad, CA, USA) were incubated with 10  $\mu\text{g}$  LEAF purified anti-human CD63 antibody (Biolegend, San Diego, CA, USA) for 30 min at RT and then rotated overnight at RT after bringing the volume to 500  $\mu\text{l}$  with 1 $\times$  PBS. Afterwards, latex bead/anti-CD63 complex were blocked with 5% BSA (Roche, Basel, Switzerland) containing 1 $\times$  PBS for 4 h at RT. Coated and blocked beads were washed twice with 1 $\times$  PBS by centrifuging at 3000 g for 10 min at RT. The coated beads were stored in 1 $\times$  PBS containing 0.1% glycine and 0.1% NaN<sub>3</sub> (@pH; 7.2) at a final concentration of  $3 \times 10^{-5}$  beads  $\mu\text{l}^{-1}$  at 4°C until analysis. Then, 1  $\mu\text{g}$  exosomal protein containing intact EVs were incubated with 1  $\mu\text{l}$  of anti-CD63 coated beads in 100  $\mu\text{l}$  FACS Buffer (FB; 1 $\times$  PBS containing 5% BSA and 0.05% Tween 20) with gentle mixing for 30 min at RT. EV bound beads were centrifuged at 3000 $\times$ g for 10 min and supernatant was removed. Beads were washed twice with FB. After that exosome/bead complex were incubated with anti-CD9-PE, CD63-PE antibody (Biolegend) or Annexin V-PE (AnV, Becton Dickinson, Franklin Lakes, NJ, USA) in FB or in 1 $\times$  BB, respectively, for 30 min with gentle mixing at RT. At the end of incubation period, EV/bead complexes were centrifuged, washed twice and analysed by BD Accuri C6 (Becton Dickinson) flow cytometer.

### **Determination of size distribution of EVs by dynamic light scattering**

Hydrated sizes of EVs isolated from healthy donors and BD patient plasmas were 100 $\times$  diluted with 1 $\times$  PBS and analysed by dynamic light scatter method on Zetasizer (Nano ZS, Malvern Instruments, Malvern, UK).

### **Isolation of exosomes from blood plasma with size exclusion chromatography**

For isolation of exosomes with size exclusion chromatography (SEC), plasma samples (1–1.5 ml) from Behçet's patients or healthy donors were diluted up to 2 ml with PBS and centrifuged at 10,000g for 20 min to get rid of debris and precipitates. The supernatants were

collected, filtered through 0.22  $\mu\text{m}$  filters and subsequently loaded on a HiPrep 16/60 Sephacryl S-400 HR SEC column (GE Healthcare, Uppsala, Sweden) with a 120 ml bed volume connected to an ÄKTA FPLC system (GE Healthcare). The separation was done at a 0.5 ml  $\text{min}^{-1}$  flow rate using PBS as the eluent while the chromatogram was recorded using absorbance at 280 nm and 2 ml fractions were collected. After separation, the indicated fractions were pooled and concentrated using ultracentrifugation as described above.

### **Flow cytometer analyses of labelled EVs**

For the identification and quantification of EVs, samples were double-stained with AnV (-PE or FITC conjugated, Biolegend) and an antibody against one of the following cell surface markers: PE-CD42a (platelet, BD Pharmingen, Franklin Lakes, NJ, USA), FITC-CD31 (endothelial cells, Biolegend), PE-CD69 (early activated cells, Biolegend) PE-CD105 (epithelial/endothelial cells, Biolegend), PE-CD3 (T-cells, BD Pharmingen) and PE-CD14 (monocytes, BD Pharmingen). Then 25  $\mu\text{l}$  EVs aliquots were incubated with a staining cocktail containing of 5  $\mu\text{l}$  AnV (as instructed in the manufacturers protocol) and 1  $\mu\text{g}$   $\text{ml}^{-1}$  of one of the indicated cell surface markers) for 30 min at RT in dark. Following staining, EVs were washed by ultracentrifugation and then dissolved in 500  $\mu\text{l}$  of 1 $\times$  BB, particles were counted on a FACS Calibur (Becton Dickinson) flow cytometer using a 60 s acquisition time at a “medium-flow” setting and data evaluation was performed using the CellQuest Pro Software (Becton Dickinson). Of note, in order to gate-out air bubbles, electrical noise and contaminating particles, a very stringent FSC-SSC gating strategy was used as indicated by the “EV-associated particle gate” (Supplementary Figure 2). In addition, to gate out particles >1  $\mu\text{m}$ , latex beads (Sigma LB-11, St. Louis, MO, USA) with 1.1  $\mu\text{m}$  diameter were used to define our EV associated gate. The optimised acquisition settings were controlled weekly. In some experiments, data acquisition was performed on an Accuri C6 Flow cytometer with similar results to those obtained using the FACS Calibur.

### **Calculation of EV number in one ml plasma**

Our initial optimisation studies were performed with standard calibration beads of known concentration ( $1 \times 10^7$  beads  $\text{ml}^{-1}$ , Sigma LB-11, 1.1  $\mu\text{m}$  in diameter). We acquired the # of events (@ 1 min) and determined the volume utilised for that run. After verification, we acquired AnV positive EVs and multiplied with the dilution factor to determine the # of EVs  $\text{ml}^{-1}$  plasma.

### Binding and uptake of EVs by PBMCs

Purified EVs were stained with the lipophilic cell tracers of CM-Dil (for confocal studies) and SP-DiOC (for binding and uptake studies) at 1  $\mu\text{M}$  concentration by incubating for 30 min at 37°C and then washed two times in 35 ml PBS and centrifuged at 100,000g for 1 h. As a negative control, 1  $\mu\text{M}$  dye, both for CM-Dil and SP-DiOC, was incubated in the absence of EVs and then washed twice. Following re-suspension in 200  $\mu\text{l}$  of endotoxin-free PBS, labelled EVs were incubated with  $2 \times 10^6 \text{ ml}^{-1}$  PBMCs at the 1:2 cell:EV ratio. For binding and uptake studies, cells were incubated with SP-DiOC labelled EVs for various time points and cells were analysed by Accuri C6 flow cytometer. For confocal microscopy studies, cells were incubated on cover slips with CM-Dil labelled EVs for 8 h (at 1:2 cell:EV ratio), washed, fixed and studied using a Zeiss LSM5 (Carl Zeiss, Oberkochen, Germany) confocal microscope.

### Human ELISA studies

EVs from active BD, inactive BD and healthy subjects were incubated with healthy PBMCs and autologous PBMCs ( $1.25 \times 10^6$  per ml) for 12 h at a ratio of 1:2 (Cell:EV) in 96-well flat bottom culture plates. In some experiments, healthy EVs were mixed with recombinant LL37 (AnaSpec, Fremont, CA, USA) overnight and incubated with autologous PBMCs for 12h. In neutralization studies anti-LL37 mAb (HyCult Biotech, Uden, Netherlands) were incubated with EV treated PBMCs at indicated concentrations. LPS ( $5 \mu\text{g ml}^{-1}$ ) and PGN ( $5 \mu\text{g ml}^{-1}$ ) were used as positive controls throughout these assays. Culture supernatants were collected and IL6 production was determined by ELISA.[34] The concentration of LL37 from plasma and EV samples was measured by a human LL37 ELISA kit (HyCult Biotech), according to the manufacturer's protocol.

### Intracellular cytokine staining

Healthy EVs with or without LL37 were used to stimulate healthy PBMCs for determining IP10, IL1 $\beta$  and IFN $\alpha$  positive cells. Healthy PBMCs were stimulated with EV or EV/LL37 complex for 6 h and 16 h in the presence of Brefeldin-A ( $5 \mu\text{g ml}^{-1}$ , Biolegend, Cat#420601) for IL1 $\beta$  and IP10 analysis, respectively. Of note, Brefeldin-A was added at  $t = 0$  and  $t = 6$ th hour of incubation for IL1 $\beta$  and for IP10, respectively. The cells were then fixed with Fix & Perm Medium A (Invitrogen, Cat# GAS001S100). Cells were first stained with CD14-PE (Biolegend, Cat#325606) and then to detect the level of intracellular IL1 $\beta$  or IP10 were stained with IL1 $\beta$ -FITC (e-

Biosciences, Cat# 12-7018-81) or IP10-Biotin (BD, Cat# 555048) then SA-FITC (Biolegend, Cat# 405202) in the presence of saponin (0.1%).

IFN $\alpha$  secreting cells were analysed with Miltenyi Biotech's (San Diego, CA, USA) IFN $\alpha$  Secretion Assay and Detection Kit (PE-labelled, Miltenyi, Cat# 130-094-161) from PBMCs in accordance with kit instructions. Additionally, in order to identify IFN $\alpha$  secreting pDCs, cells were stained with BDCA-2-FITC (Biolegend, Cat# 354208) and then analysed by BD Accuri C6 flow cytometer.

### Statistical analysis

All statistical data analyses were carried out using the Sigma Stat 3.5 (Systat Software Inc., London, UK). In order to assess significance between active BD, inactive BD and healthy groups, one-way ANOVA test was used, while Student's t-test was applied to analyse significance between sub-groups of active BD vs. inactive BD.  $p$ -values  $\leq 0.05$  were set to be statistically significant.

## Results

### Characterisation of EVs from blood plasma

We collected EVs following either ultracentrifugation or sucrose cushion and conducted Western blotting analyses. The exosome marker proteins Alix, and Grp94 were detected in EVs purified from plasma (Supplementary Figure 1(a)). Furthermore, via bead-based flow cytometric analysis, we demonstrated that EVs express cardinal markers such as CD9 and CD63 (Supplementary Figure 1(b)). Moreover, isolated EVs were subjected to dynamic light scattering analyses to determine the size distribution. DLS investigation revealed that the size of the purified EVs from healthy or BD patient plasmas following ultracentrifugation or sucrose cushion were in the expected size range (ranging between  $\sim 30$  and 1000 nm, Supplementary Figure 1(c)).

### BD patients have elevated circulating EV numbers

To assess whether plasma EV concentrations correlated with BD severity, EV numbers in plasma of 72 BD patients (active;  $n = 35$ , inactive;  $n = 37$ ) and 22 healthy controls were determined by flow cytometry. Results presented in Figure 1 show that total plasma EV concentrations (number of EV  $\text{ml}^{-1}$  plasma) were significantly higher in active BD ( $3.9 \pm 0.77 \times 10^5$ ) and inactive BD ( $2.05 \pm 0.46 \times 10^5$ ) compared to healthy plasma EVs ( $0.78 \pm 0.25 \times 10^5$ ,  $p < 0.001$ , active vs. healthy, and inactive vs. healthy). Total EV numbers in active BD were consistently higher

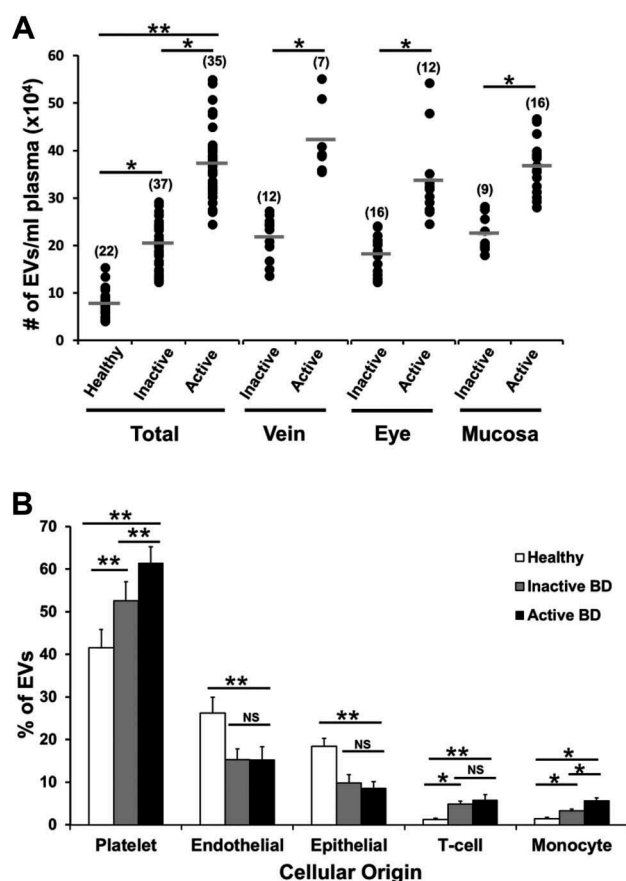


**Figure 1.** Differential levels and cellular origin of EVs in BD plasma. (a) Plasma EVs were purified and stained with AnV-FITC as described in the Materials and Methods section. Number of EVs per ml plasma was calculated following flow analyses of AnV positive EV signals. Numbers in parentheses represent number of subjects studied. (b) EVs were stained with corresponding cell type specific surface markers as well as AnV. Data are represented as the mean percentage of AnV positive EVs derived from each cell type  $\pm$  SD for all samples. Individual dot-plots were used to calculate CD3 (T-cells), CD14 (monocytes), CD42a (platelets), CD31 (endothelial cells) and CD105 (epithelial cells) derived EV ratios over total EVs from healthy ( $n = 22$ ), inactive BD ( $n = 37$ ) and active BD ( $n = 35$ ) donors. \* $p < 0.01$  and \*\* $p < 0.001$  for comparison groups based on Student's t-test analyses of healthy vs. inactive BD, healthy vs. active BD and inactive BD vs. active BD. NS indicates not significant.

than the inactive BD group ( $p < 0.01$ ) and this increase (1.75–2.2-fold) was valid in all patient sub-groups, suggesting that elevated EV levels was a common feature of active disease and was not dependent on organ involvement (Figure 1(a),  $p < 0.01$  for all tested sub-groups).

### Platelet derived EVs constitute the majority of circulating EVs in BD plasma

EVs are believed to be secreted from multiple cell types, including platelets, endothelial cells, monocytes,

and T cells. However, contribution of each population to the circulating EV pool can vary depending on disease activity. To elucidate whether source of EVs varied with respect to BD severity, isolated particles from healthy ( $n = 22$ ), inactive ( $n = 35$ ) and active BD patients ( $n = 37$ ) were stained with different cell specific markers and their relative ratios were confirmed by flow cytometry. The gating strategy for flow cytometric analysis and representative dot-plots of individual plasma EV staining are detailed in Supplementary Figure 2 and Supplementary Figure 3. Flow cytometric analysis of stained EV populations revealed that platelets were the most common source of EV population in all groups (Figure 1(b)). Platelet-derived EV percentages correlated with disease state and were found to be significantly elevated in BD patients ( $52.6 \pm 4.5\%$  and  $65.4 \pm 3.8\%$ , inactive and active BD, respectively) when compared to healthy controls ( $41.5 \pm 4.3\%$ ,  $p < 0.001$  for all comparisons). Similarly, significant increases were found for EVs derived from T cells (Figure 1(b),  $1.49 \pm 0.36$ ,  $4.14 \pm 0.77$  and  $5.25 \pm 1.24\%$  for healthy, inactive and active BD, respectively;  $p < 0.001$ ) and monocytes (Figure 1(b),  $1.39 \pm 0.32$ ,  $3.27 \pm 0.42$  and  $5.7 \pm 0.56\%$  for healthy, inactive and active BD, respectively;  $p < 0.001$ ). In contrast, endothelial and/or epithelial derived EVs in BD plasma were lower than those observed in healthy plasma ( $p < 0.001$  for all comparisons).

### EVs are internalised by PBMCs triggering IL6 secretion

The underlying reasons for the heightened and sustained immune activation in BD patients remain elusive. We established that circulating EV concentrations are elevated, especially in active BD plasmas. We next attempted to explore the role of heightened EV concentration as a culprit in sustained immune activation in BD patients. To test this possibility, we investigated the EV internalisation using fluorescently labelled extracellular vesicles. For this, lipophilic CM-DiI dye labelled EVs were incubated with healthy PBMCs and their associations were analysed by confocal microscopy (Figure 2(a)). Photomicrographs revealed that BD EVs were effectively associated with immune cells (Figure 2(a)). This association is not mediated by non-specific binding of EVs to PBMCs because there was no cellular staining following incubation of EVs with cells at 4°C. The signal was EV specific as there was no non-specific dye binding to cells upon incubating centrifuged CM-DiI dye pellet with cells (Figure 2(a), middle and lower panels). We next attempted to explore

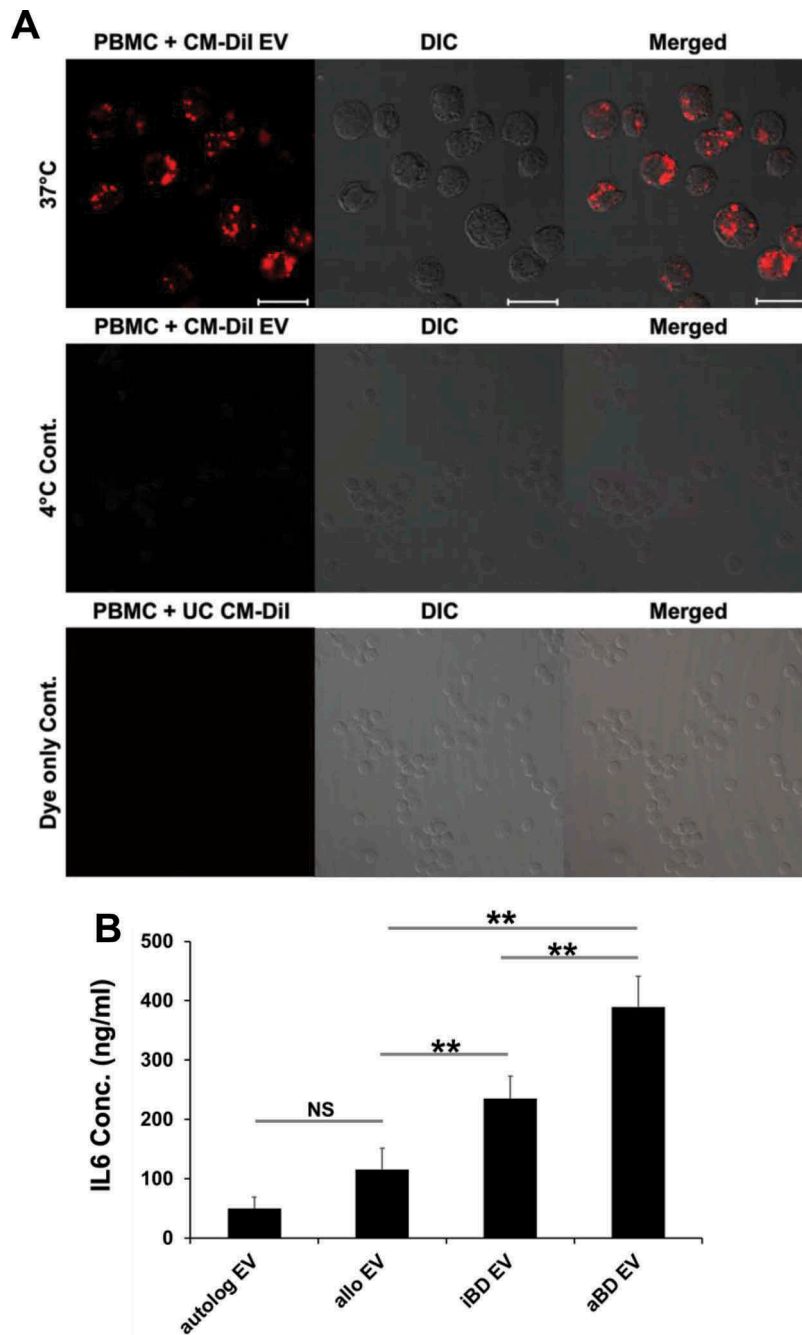


**Figure 2.** BD EV binding and IL6 secretion by PBMCs. (a) Confocal images showing interaction of EVs following 8 h of incubation with PBMCs. The upper panel shows incubation at 37°C. The middle panel is the interaction of stained EVs with cells at 4°C. The lower panel is the negative control which indicates there is no interaction of the precipitated dye following ultracentrifugation. The left panel represents CM-Dil positive signal; the middle panel represents DIC images of the cells and the right panel shows merged images (scale bar = 20  $\mu$ m). (b) Healthy PBMCs were incubated with autologous or allogeneic EVs at a cell:EV ratio of 1:2 for 12 h. IL6 production was assessed from the culture supernatants by ELISA. (autolog EV; autologous EVs from healthy donor; allo EV; allogeneic EVs from healthy donor; iBD EV; inactive BD EVs and aBD EV; active BD EVs).  $n = 12$  samples,  $**p < 0.001$  for all comparisons.

whether active BD EVs were capable of triggering an immune response. We incubated EVs isolated from healthy, inactive or active BD with healthy PBMCs for 12 h and determined EV-induced cytokine secretion from culture supernatants. Results revealed that

autologous and allogeneic healthy plasma-derived EVs triggered lower but detectable levels of IL6 production from healthy PBMC (Figure 2(b),  $49.9 \pm 19.0$  and  $116.1 \pm 35.4$  ng ml<sup>-1</sup>, respectively). In contrast, inactive and active BD patients' EVs triggered 2-fold and 3.3-

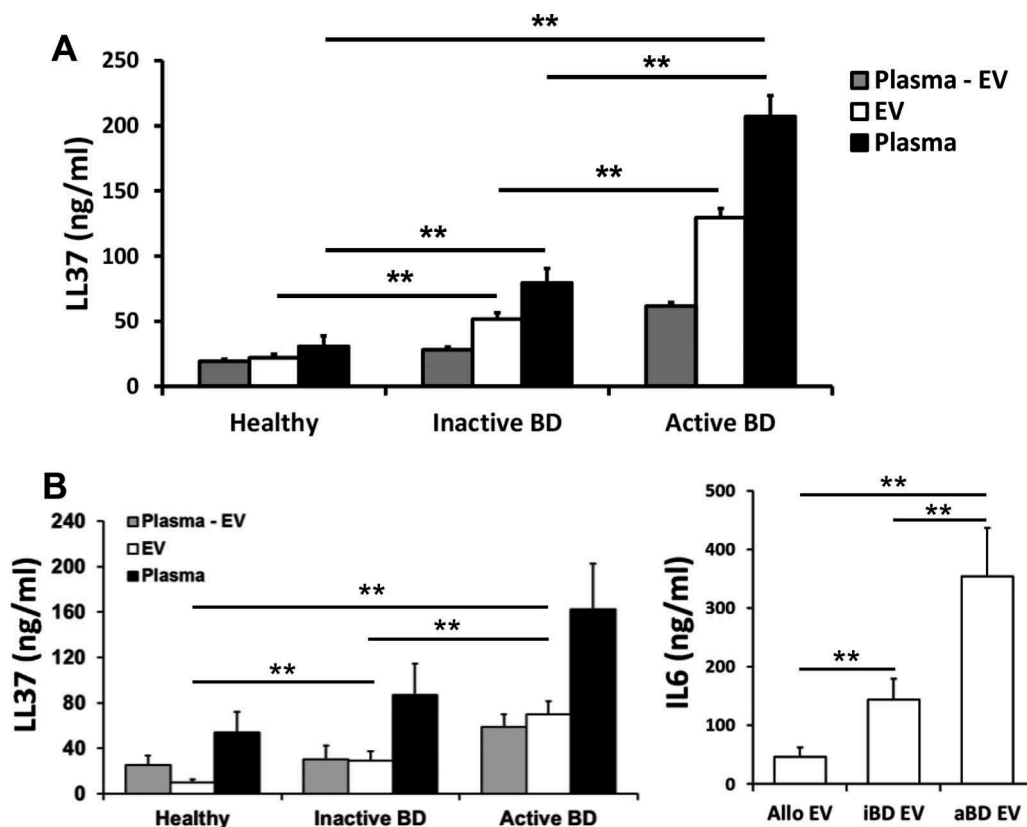


**Figure 3.** Elevated levels of antimicrobial peptide LL37 are mostly associated with EVs in BD patients. (a) LL37 concentrations ( $\text{ng ml}^{-1}$ ) in EV depleted plasma, EV fraction and in plasma of BD patients and control healthy subjects were assessed by LL37 ELISA kit. (b) LL37 levels of EVs and IL6 induction capacities of EVs (alloEV-healthy EVs; iEV-inactive BD EVs and aEV-active BD EVs) from healthy PBMCs after sucrose cushion purification ( $n = 12$  for all samples and  $**p \leq 0.001$  for all comparisons).

fold more IL6 (Figure 2(b),  $235.1 \pm 38.0$  and  $384.9 \pm 51.3 \text{ ng ml}^{-1}$ , respectively) when compared to allogeneic healthy EVs ( $p < 0.001$  for all comparisons). These findings demonstrate that EVs can interact with and are internalised by human PBMCs and this interaction leads to a more pronounced IL6 production when EVs were of BD origin.

#### Active BD patient plasma LL37 levels are elevated and majority of LL37 is associated with EVs

After establishing that circulating EVs are elevated in active BD plasma and are mediating exaggerated cytokine secretion from PBMCs, we embarked on identifying the factor(s) that might contribute to BD EV-associated immune activation. For this, we analysed the plasma levels of LL37, an anti-microbial peptide associated with the pathogenesis of several autoimmune/inflammatory diseases, including psoriasis, systemic lupus erythematosus, rheumatoid arthritis and atherosclerosis.[35] LL37 concentrations were found to be  $39 \pm 8$ ,  $80 \pm 11$  and  $207 \pm 16 \text{ ng ml}^{-1}$  in healthy, inactive and active BD plasma samples, respectively

(Figure 3(a)), representing a 2-fold (inactive) and 5-fold (active) increase.

Considering that LL37 is a cationic peptide and EVs are enriched in negatively charged phospholipids such as phosphatidyl serine [36], we next analysed the possibility of EV/LL37 interaction and determined the levels of LL37 in EV-depleted plasma and in the EV fraction following ultracentrifugation of donor plasmas. Strikingly,  $\sim 2/3$  of LL37 was found to be associated with EVs in active BD (Figure 3(b)).

To further purify EV preparations, we applied EV pellets (following ultracentrifugation) onto sucrose cushion. From this fraction, LL37 detection by ELISA was performed. As seen in Figure 3(c), LL37 level of EVs isolated from active BD plasma were significantly higher than inactive BD EVs or healthy plasma EVs ( $9.8 \pm 3$ ;  $29.1 \pm 8.6$ , and  $70.6 \pm 11.2 \text{ ng ml}^{-1}$  LL37 in healthy, inactive BD and active BD EVs, respectively,  $n = 12$  for each samples,  $p < 0.001$ ). Furthermore, consistent with previous findings provided in Figure 2 (b), active BD EVs induced significantly higher IL6 secretion than inactive BD EVs and healthy EVs (Figure 3(c), right panel,  $p < 0.001$ ). Collectively,



these findings implied that EVs are associated with LL37 and are capable of inducing IL6 secretion from healthy PBMCs (Figure 3(c)).

In order to further rule out contribution of unassociated LL37 aggregates to observed immune activation, we additionally subjected plasma from healthy and active BD patients to size exclusion chromatography purification (SEC) (Supplementary Figure 4(a)). The SEC fractions were then analysed for expression of cardinal EV markers via the bead method and each fraction was analysed by flow cytometer (Supplementary Figure 4(b)). As expected, EV markers such as CD9 and CD63 were highly abundant only in fraction #1 (>2–2.5-fold more marker expression) coinciding only to the EV fraction, compared to other fractions as expected, suggesting the presence of EVs in this fraction (Supplementary Figure 4(b)). Furthermore, LL37 levels of each fraction was analysed by ELISA and found to be significantly higher in the SEC fraction #1, thereby coinciding with the EVs (Supplementary Figure 4(c), SEC Fraction #1:  $58.9 \pm 7.1$ ; SEC Fraction #2:  $5.7 \pm 1.9$ , and SEC Fraction #3:  $21.6 \pm 2.7$  ng ml<sup>-1</sup>). Lastly, we checked the IL6 induction potential of each SEC fraction. Following incubation of fractions with healthy PBMCs for 12 h in culture, data revealed that significantly higher levels of IL6 was obtained only from cell supernatants that was treated with active BD derived plasma fraction #1 compared to healthy EV fractions. Furthermore, only fraction #1 of active BD plasma induced IL6 secretion compared to fraction #2 and fraction #3 ( $185.4 \pm 30.9$  ng ml<sup>-1</sup>,  $28.6 \pm 7.5$  ng ml<sup>-1</sup>, and  $49.1 \pm 14.1$  ng ml<sup>-1</sup>, for SEC Fraction #1, #2, and #3, respectively) (Supplementary Figure 4(d),  $p < 0.001$ ).

### **LL37 association with EV governs cellular internalisation and cytokine induction**

LL37 was previously shown to interact with and enhance delivery of nucleic acids to immune cells.[37] To assess whether a similar mechanism could operate for EVs, SP-DiOC labelled healthy EVs were either used as such or mixed with LL37 peptide (endotoxin free) prior to incubation with healthy donor PBMCs (Figure 4). Binding of EVs was significantly enhanced when PBMCs were incubated with LL37 associated EVs. This enhanced binding was much pronounced when incubation period was extended to 8 h (Figure 4(a) and Supplementary Figure 5,  $p < 0.001$ , EV vs. EV + LL37 comparison).

Next, to establish whether this enhanced LL37-mediated cellular internalisation had an impact on subsequent cytokine induction, healthy EVs were mixed with increasing concentrations of LL37 or its scrambled-control prior to co-culture with healthy

PBMCs. As seen in Figure 4(b), LL37/EV combination induced significantly higher IL6 secretion from PBMCs in a dose dependent manner ( $p < 0.001$ ). This induction was specific to LL37 since the scrambled peptide (SCR/EV) combination did not yield appreciable amounts of IL6 (Figure 4(b)). Although free LL37 also triggered IL6 release at these doses, EV/LL37 combination triggered 2.2–2.3-fold more IL6 than the free peptide at both doses (150 and 450 ng, respectively, Figure 4(b)). To further demonstrate that any contaminating LL37 aggregate together with EVs does not contribute to IL6 production by PBMCs, we conducted an additional experiment using THP1 cell derived EVs. We isolated EVs from THP1 cell supernatants that were devoid of any plasma components and complexed with LL37 as described earlier and incubated with PBMCs. As done previously, IL6 production by PBMCs was assessed by ELISA. As seen in Figure 4(c), EV/LL37 treated PBMCs secreted more IL6, representing a 2.1-fold higher cytokine production compared to cells that were treated with free LL37 (Figure 4(c)). Consistently, scrambled peptide mixed EVs failed to secrete any appreciable levels of IL6. To further prove that indeed LL37 association to EVs regulates cytokine induction by PBMCs, next, we treated cells with EV/LL37 complex in the presence and absence of anti-LL37 antibody and detected IL6 levels from cell supernatants. As seen in Figure 4(d), in a dose-dependent manner anti-LL37 addition onto LL37-EV treated cells significantly abrogated IL6 secretion from PBMCs suggesting that LL37/EVs regulate IL6 secretion from PBMCs (Figure 4(d)). Of important note, IL6 secretion capacity of EVs isolated from inactive and active BD patient plasmas significantly reduced when increasing doses of anti-LL37 antibody was incubated with healthy PBMCs (Supplementary Figure 5(b)).

### **Active BD EVs triggers IFN $\alpha$ from pDC, IL1 $\beta$ and IP10 from monocytes/macrophages**

Our findings implicated that LL37 associated EVs are capable of inducing elevated immune activation. To identify the cell types activated by LL37/EV complexes, healthy donor EVs were mixed with LL37, (mimicking active BD EVs) and subsequently incubated with healthy PBMCs. LL37-free and LL37 associated-EV binding profiles in dendritic cell (DC), macrophage and T-cell populations were assessed with flow cytometer 1 h after co-incubation (Figure 5 and Supplementary Figure 5(a)). Results showed that EV delivery to macrophages, DCs and to a lesser extent to T-cells were significantly enhanced in the presence of LL37 (Figure 5(a)).

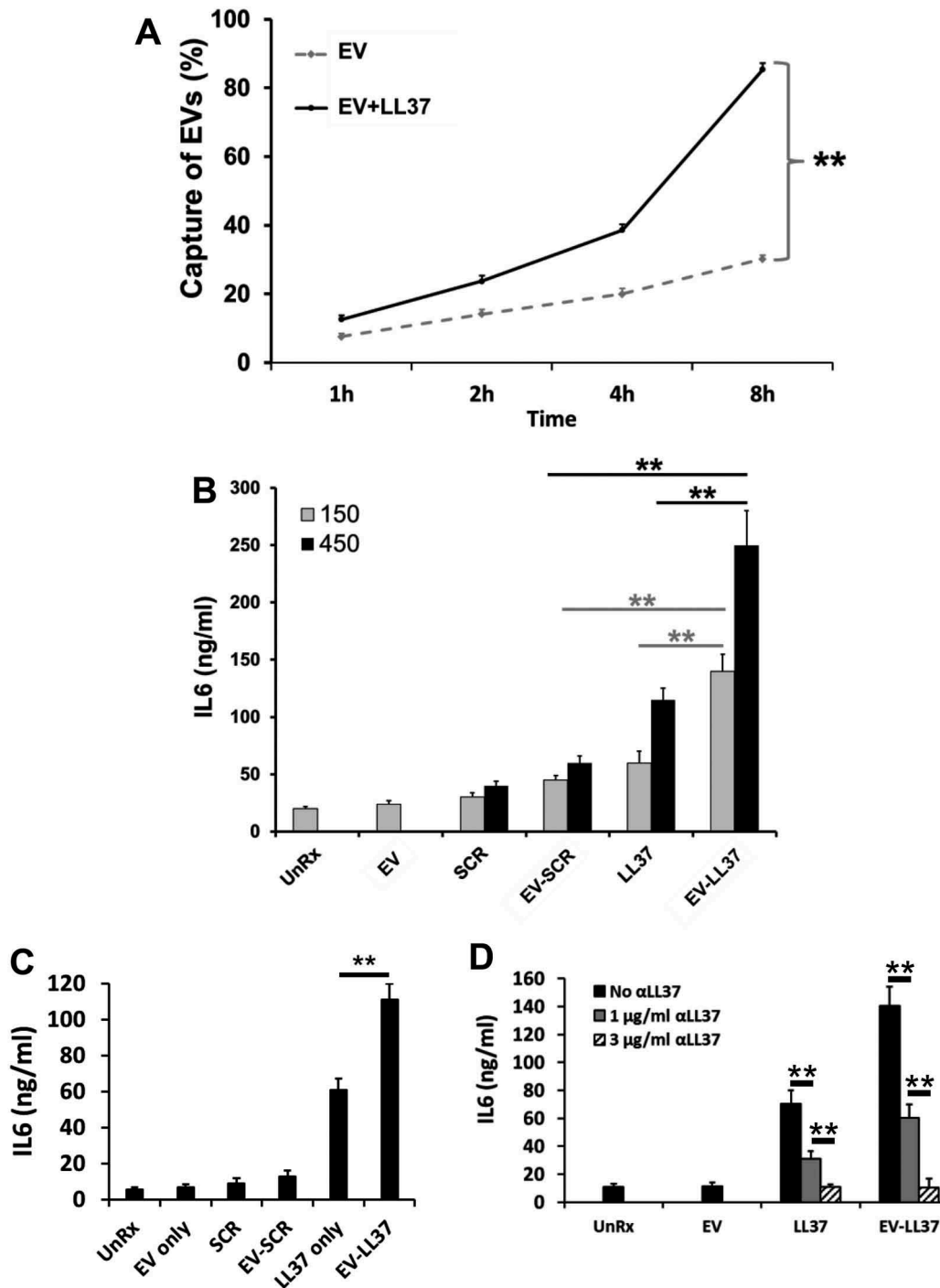


**Figure 4.** LL37 promotes EVs uptake and IL6 induction by immune cells can be suppressed by LL37 antibody. (a) SP-DiOC labelled healthy EVs or LL37/EV complexes were incubated with healthy PBMCs at 1:2 ratio (cell:EV) for indicated time periods. The line graph shows the kinetic of EVs association by cells in the presence or absence of LL37. (b) EVs isolated from healthy plasma were complexed overnight at 4°C either with 150 ng (grey bars) or with 450 ng (black bars) LL37, and then incubated with healthy PBMCs for 12 h at 1:2 (cell:EV) ratio. IL6 levels were assessed from culture supernatants by ELISA. (c) IL6 induction capacity of EVs isolated from THP-1 cells that is devoid of any plasma contamination. (d) Dose-dependent suppression of LL37/EV mediated IL6 production by PBMCs following treatment with anti-LL37 antibody for 12 h in culture.  $**p < 0.001$  for all comparisons.

Next, EV mediated immune activation by blood peripheral cells were investigated. As expected, healthy EVs devoid of LL37 failed to induce any detectable IFN $\alpha$  or IL1 $\beta$  (Figure 5(b), and Supplementary Figure 6).

However, LL37/EV complexes induced >2-fold more IL1 $\beta$ , and >20-fold more IFN $\alpha$  production from monocytes and plasmacytoid dendritic cells (pDC), respectively. Similarly, IP10 production from monocytes was

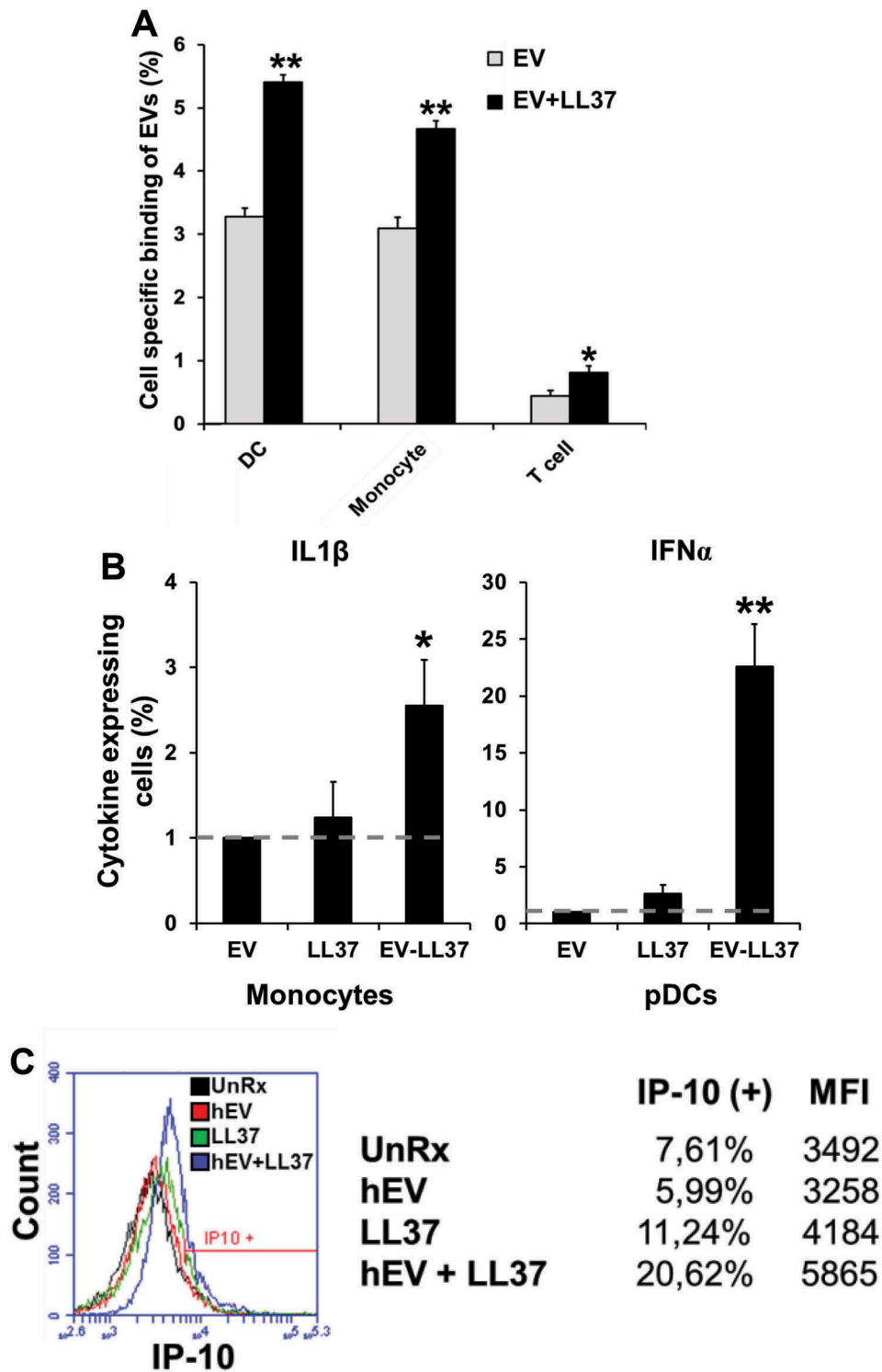


**Figure 5.** EVs associated with LL37 can be taken up by immune cells and boost IL1 $\beta$  and IP10 from monocytes and IFN $\alpha$  from pDCs. (a) Cell specific binding of LL37-free and LL37-associated EVs. SP-DiOC stained EVs were incubated with PBMCs for 1 h and analysed by flow cytometer following cell-specific surface marker staining. (b) IL1 $\beta$  and IFN $\alpha$  secreting monocytes and pDCs, respectively, were assessed by intracellular cytokine staining technique. (c) Histogram of IP10 secreting monocytes were shown following treatment of cells either with EVs or free LL37 and LL37/EV complex.

elevated only in response to LL37-EV (Figure 5(c), >2-fold more IP10 was secreted). Of note, IFN $\alpha$ , IL1 $\beta$  and IP10 productions from pDC and monocytes were

dependent on LL37-EV complex since treatment of cells only with LL37 failed to reproduce similar immune stimulatory activity.

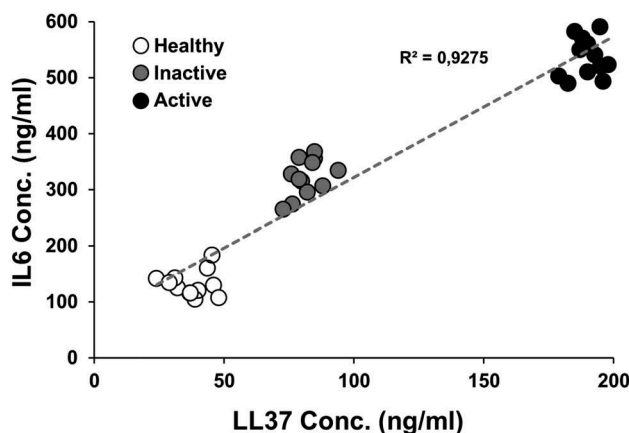


**Figure 6.** Disease activity strongly correlates with LL37 and IL6 concentrations. Healthy, inactive and active BD patient EVs were analysed for LL37 association levels and subsequent IL6 production by healthy PBMCs. The correlation plot was prepared from these two independent data to determine the correlation coefficient between disease states IL6 secretion and LL37 levels.  $R^2 =$  coefficient of correlation ( $n = 12$  for all sample plasmas).

When taken together, these findings demonstrated that (i) LL37 levels, (ii) EVs concentration and (iii) pathological cytokine production are well correlated with disease severity (Figure 6,  $R^2$ : 0.9275, and Supplementary Figure 7(a) and 7(b)).

Collectively, our findings established that active BD patient plasmas contain elevated numbers of circulating EVs, and majority of LL37 does not co-exist in the EV pellet as a contaminating aggregate but are physically associated with LL37. The EV-LL37 complex drives EVs specifically and efficiently to immune cells, probably inducing robust and sustained immune activation.

## Discussion

EVs have recently been implicated as novel extracellular mediators of distant intercellular communication. [11] Since EVs circulate and remain intact in peripheral blood, they are capable of transferring labile cargo to distant targets, thereby altering the physiology of the recipient cells. This study is the first to demonstrate that EVs are elevated in the peripheral blood of BD patients, suggesting their potential involvement in disease pathogenesis.

Several studies demonstrated that EVs not only possess bioactive materials on their surface but also harbour biologically active cargo within their lumen. These include nucleic acids (both RNA and DNA) or proteins, such as cytokines, growth factors and cell or tissue specific antigens. Recently, miRNAs were also reported to be delivered via these structures.[38–40] EVs are considered

to have important functions in establishment of homeostasis in health and could play potentially detrimental roles during disease states.[41,42] Data presented herein are in support of these observations and extend our current knowledge of EV-disease associations.

Several concerns could be raised during working with plasma in an EV related study, such as contamination of EVs during the isolation step with several other unrelated proteins or protein aggregates that ultimately overshadow the anticipated results. Importantly, the presence of negatively charged apolipoproteins in EV pellets as a contaminant could facilitate association of cationic plasma LL37 with apolipoproteins. However, according to two studies, this association abrogates LL37 inherent immune related activity.[43,44] Since we purified EVs also on a sucrose cushion, we consider it unlikely that apolipoprotein mediated LL37 complexes contributed to the activities observed by EV-LL37.

Our findings could be of clinical interest for several reasons. First, plasma EV numbers were found to be elevated in BD patients, which correlated with disease severity (higher EV numbers in active BD patients). It is conceivable that a plasma EV number-based stratification of BD could more precisely identify inactive and active disease states and could aid in pharmacological management of this disease.

Second, although LL37 is a cationic anti-microbial peptide generally known to be secreted during pathogenic insult,[45–47] the data presented here demonstrate that plasma LL37 levels are elevated in BD. As in the case of EVs, this information could be of value to follow patient responses to treatment. Of interest, the only published data that investigated a role of LL37 in BD revealed elevated LL37 levels in saliva of BD patients which correlated with the number of monthly oral ulcers.[48] Consistent with this observation, our results also revealed a correlation between LL37 levels and disease severity. Of note, LL37 levels were reported to be higher during sterile inflammation.[49] In addition, this cationic peptide was demonstrated to contribute to IL-1 $\beta$ , IL6, MCP-1 and MCP-3 production.[50] In this context, our results also established a link between elevated LL37 levels and enhanced cytokine production.

Third, to our knowledge this paper is the first to show that LL37 can interact with EVs, enhancing their cellular delivery and immune stimulatory activity. As stated before, EVs are known carriers of self-nucleic acids. It is conceivable that LL37-mediated enhanced EV delivery to immune cells could activate several endosomal and/or cytosolic RNA and DNA-dependent nucleic acid sensors, including TLR7, TLR9, RIG-I, MDA-5, cGAS or AIM-2, leading to production of

BD-associated cytokines (i.e. IL6, IL-1 $\beta$  and IFN $\alpha$ ), contributing to disease severity. Supporting this view, it was shown that high levels of LL37 present in psoriatic skin formed complexes with genomic DNA liberated from dying cells, and enhanced DNA delivery to pDCs, triggering a TLR9-mediated interferon alpha response in psoriatic patients.[51]

The anionic charge of EVs provides a surface convenient for complexing with LL37. Our findings imply that LL37-mediated enhanced delivery of circulating EVs to immune cells contributes to sustaining and exacerbating immune activation in active BD. Therefore, targeting this peptide could be of therapeutic value in the management of this complex disease.

### Acknowledgements

Dr Gizem Tincer Konig and Deniz C. Kahraman are sincerely acknowledged for their critical reading of the manuscript and feedback during the study.

### Disclosure statement

No potential conflict of interest was reported by the authors.

### Funding

This work is partially supported by a TUBITAK grant [SBAG: 108S316]. Tamer Kahraman received scholarship from Scientific and Technological Research Council of Turkey [TUBITAK grant number 108S316].

### References

- [1] Comarmond C, Wechsler B, Bodaghi B, et al. Biotherapies in Behcet's disease. *Autoimmun Rev*. 2014;13:762–769.
- [2] Hatemi G, Merkel PA, Hamuryudan V, et al. Outcome measures used in clinical trials for Behcet syndrome: a systematic review. *J Rheumatol*. 2014;41:599–612.
- [3] Direskeneli H. Autoimmunity vs autoinflammation in Behcet's disease: do we oversimplify a complex disorder? *Rheumatology*. 2006;45:1461–1465.
- [4] Emmi G, Silvestri E, Squatrito D, et al. Behcet's syndrome pathophysiology and potential therapeutic targets. *Intern Emerg Med*. 2014;9:257–265.
- [5] Yazici Y, Yurdakul S, Yazici H. Behcet's syndrome. *Curr Rheumatol Rep*. 2010;12:429–435.
- [6] Hamzaoui K, Hamzaoui A, Guemira F, et al. Cytokine profile in Behcet's disease patients. Relationship with disease activity. *Scand J Rheumatol*. 2002;31:205–210.
- [7] Hatemi G, Yazici Y, Yazici H. Behcet's syndrome. *Rheum Dis Clin North Am*. 2013;39:245–261.
- [8] Melikoglu M, Uysal S, Krueger JG, et al. Characterization of the divergent wound-healing responses occurring in the pathergy reaction and normal healthy volunteers. *J Immunol*. 2006;177:6415–6421.
- [9] Raziuddin S, Al-Dalaan A, Bahabri S, et al. Divergent cytokine production profile in Behcet's disease. Altered Th1/Th2 cell cytokine pattern. *J Rheumatol*. 1998;25:329–333.
- [10] Raizman MB, Foster CS. Plasma exchange in the therapy of Behcet's disease. *Graefes Arch Clin Exp Ophthalmol*. 1989;227:360–363.
- [11] Distler JH, Huber LC, Gay S, et al. Microparticles as mediators of cellular cross-talk in inflammatory disease. *Autoimmunity*. 2006;39:683–690.
- [12] Théry C, Ostrowski M, Segura E. Membrane vesicles as conveyors of immune responses. *Nat Rev Immunol*. 2009;9:581–593.
- [13] Distler JH, Jungel A, Huber LC, et al. The induction of matrix metalloproteinase and cytokine expression in synovial fibroblasts stimulated with immune cell microparticles. *Proc Natl Acad Sci U S A*. 2005;102:2892–2897.
- [14] Barry OP, Praticò D, Savani RC, et al. Modulation of monocyte-endothelial cell interactions by platelet microparticles. *J Clin Invest*. 1998;102:136–144.
- [15] Duval A, Helley D, Capron L, et al. Endothelial dysfunction in systemic lupus patients with low disease activity: evaluation by quantification and characterization of circulating endothelial microparticles, role of anti-endothelial cell antibodies. *Rheumatology (Oxford)*. 2010;49:1049–1055.
- [16] Ullal AJ, Pisetsky DS. The release of microparticles by Jurkat leukemia T cells treated with staurosporine and related kinase inhibitors to induce apoptosis. *Apoptosis*. 2010;15:586–596.
- [17] VanWijk MJ, VanBavel E, Sturk A, et al. Microparticles in cardiovascular diseases. *Cardiovasc Res*. 2003;59:277–287.
- [18] Gauley J, Pisetsky DS. The release of microparticles by RAW 264.7 macrophage cells stimulated with TLR ligands. *J Leukoc Biol*. 2010;87:1115–1123.
- [19] Beyer C, Pisetsky DS. The role of microparticles in the pathogenesis of rheumatic diseases. *Nat Rev Rheumatol*. 2010;6:21–29.
- [20] Berckmans RJ, Nieuwland R, Kraan MC, et al. Synovial microparticles from arthritic patients modulate chemokine and cytokine release by synoviocytes. *Arthritis Res Ther*. 2005;7:R536–R544.
- [21] Berckmans RJ, Nieuwland R, Tak PP, et al. Cell-derived microparticles in synovial fluid from inflamed arthritic joints support coagulation exclusively via a factor VII-dependent mechanism. *Arthritis Rheum*. 2002;46:2857–2866.
- [22] Brogan PA, Shah V, Brachet C, et al. Endothelial and platelet microparticles in vasculitis of the young. *Arthritis Rheum*. 2004;50:927–936.
- [23] Brogan PA, Dillon MJ. Endothelial microparticles and the diagnosis of the vasculitides. *Intern Med*. 2004;43:1115–1119.
- [24] Combes V, Simon AC, Grau GE, et al. In vitro generation of endothelial microparticles and possible prothrombotic activity in patients with lupus anticoagulant. *J Clin Invest*. 1999;104:93–102.
- [25] Guiducci S, Distler JH, Jungel A, et al. The relationship between plasma microparticles and disease manifestations in patients with systemic sclerosis. *Arthritis Rheum*. 2008;58:2845–2853.

- [26] Knijff-Dutmer EA, Koerts J, Nieuwland R, et al. Elevated levels of platelet microparticles are associated with disease activity in rheumatoid arthritis. *Arthritis Rheum.* 2002;46:1498–1503.
- [27] Larkin M. Raised endothelial microparticles an early marker for multiple sclerosis? *Lancet.* 2001;357:1679.
- [28] Minagar A, Jy W, Jimenez JJ, et al. Elevated plasma endothelial microparticles in multiple sclerosis. *Neurology.* 2001;56:1319–1324.
- [29] Sellam J, Proulle V, Jungel A, et al. Increased levels of circulating microparticles in primary Sjogren's syndrome, systemic lupus erythematosus and rheumatoid arthritis and relation with disease activity. *Arthritis Res Ther.* 2009;11:R156.
- [30] van Eijk IC, Tushuizen ME, Sturk A, et al. Circulating microparticles remain associated with complement activation despite intensive anti-inflammatory therapy in early rheumatoid arthritis. *Ann Rheum Dis.* 2010;69:1378–1382.
- [31] Dye JR, Ullal AJ, Pisetsky DS. The role of microparticles in the pathogenesis of rheumatoid arthritis and systemic lupus erythematosus. *Scand J Immunol.* 2013;78:140–148.
- [32] Criteria for diagnosis of Behcet's disease. International study group for Behcet's disease. *Lancet.* 1990;335:1078–1080.
- [33] They C, Amigorena S, Raposo G, et al. Isolation and characterization of exosomes from cell culture supernatants and biological fluids. *Curr Protoc Cell Biol.* 2006;Chapter 3:Unit 3 22.
- [34] Gursel I, Gursel M, Yamada H, et al. Repetitive elements in mammalian telomeres suppress bacterial DNA-induced immune activation. *J Immunol.* 2003;171:1393–1400.
- [35] Kahlenberg JM, Kaplan MJ. Little peptide, big effects: the role of LL-37 in inflammation and autoimmune disease. *J Immunol.* 2013;191:4895–4901.
- [36] Lynch SF, Ludlam CA. Plasma microparticles and vascular disorders. *Br J Haematol.* 2007;137:36–48.
- [37] Hurtado P, Peh CA. LL-37 promotes rapid sensing of CpG oligodeoxynucleotides by B lymphocytes and plasmacytoid dendritic cells. *J Immunol.* 2010;184:1425–1435.
- [38] Cocucci E, Racchetti G, Meldolesi J. Shedding microvesicles: artefacts no more. *Trends Cell Biol.* 2009;19:43–51.
- [39] Hunter MP, Ismail N, Zhang X, et al. Detection of microRNA expression in human peripheral blood microvesicles. *PLoS One.* 2008;3:e3694.
- [40] Reich CF 3rd, Pisetsky DS. The content of DNA and RNA in microparticles released by Jurkat and HL-60 cells undergoing in vitro apoptosis. *Exp Cell Res.* 2009;315:760–768.
- [41] Hugel B, Martínez MC, Kunzelmann C, et al. Membrane microparticles: two sides of the coin. *Physiology (Bethesda).* 2005;20:22–27.
- [42] Yáñez-Mó M, Siljander PR, Andreu Z, et al. Biological properties of extracellular vesicles and their physiological functions. *J Extracell Vesicles.* 2015;4:27066.
- [43] Wang YQ, Johansson J, Agerberth B, et al. The antimicrobial peptide LL-37 binds to the human plasma protein apolipoprotein A-I. *Rapid Commun Mass Spectrom.* 2004;18:588–589.
- [44] Wang Y, Agerberth B, Löthgren A, et al. Apolipoprotein A-I binds and inhibits the human antibacterial/cytotoxic peptide LL-37. *J Biol Chem.* 1998;273:33115–33118.
- [45] Dean SN, Bishop BM, van Hoek ML. Susceptibility of *Pseudomonas aeruginosa* biofilm to alpha-helical peptides: D-enantiomer of LL-37. *Front Microbiol.* 2011;2:128.
- [46] Wong JH, Ng TB, Legowska A, et al. Antifungal action of human cathelicidin fragment (LL13-37) on *Candida albicans*. *Peptides.* 2011;32:1996–2002.
- [47] Barlow PG, Svoboda P, Mackellar A, et al. Antiviral activity and increased host defense against influenza infection elicited by the human cathelicidin LL-37. *PLoS One.* 2011;6:e25333.
- [48] Mumcu G, Cimilli H, Karacayli U, et al. Salivary levels of antimicrobial peptides Hnp 1-3, LL-37 and S100 in Behcet's disease. *Arch Oral Biol.* 2012;57:642–646.
- [49] Vandamme D, Landuyt B, Luyten W, et al. A comprehensive summary of LL-37, the factotum human cathelicidin peptide. *Cell Immunol.* 2012;280:22–35.
- [50] Yu J, Mookherjee N, Wee K, et al. Host defense peptide LL-37, in synergy with inflammatory mediator IL-1beta, augments immune responses by multiple pathways. *J Immunol.* 2007;179:7684–7691.
- [51] Lande R, Gregorio J, Facchinetti V, et al. Plasmacytoid dendritic cells sense self-DNA coupled with antimicrobial peptide. *Nature.* 2007;449:564–569.